Constitutive and stochastic models to predict the effect of casting defects on the mechanical properties of High Pressure Die Cast AlSi9Cu3(Fe) alloys

Giulio Timelli
Department of Management and Engineering, University of Padova, Vicenza, Italy.

ABSTRACT

The effect of casting defects on mechanical properties of a high-pressure die-cast AlSi9Cu3(Fe) alloy is reported. A series of U-shaped structural components are cast using a combination of injection parameters and pouring temperatures in order to generate different types and amount of casting defects throughout the casting. It has been found that castings contain defects, primarily pores and oxides, and that the presence and distribution of these defects are highly sensitive to the process conditions. Moreover, significant variations of the defect distribution have, however, been found in castings produced under the same conditions, indicating the stochastic nature of defects in die castings. The tensile properties are affected by the amount and distribution of defects and are determined by the defect area fraction. The influence of casting defects on mechanical properties are investigated through a theoretical verification based on constitutive and stochastic models. The analytical approach, based on the Ghosh constitutive model of tension instability, correctly indicates the trends of the experimental results, while the Weibull statistics evidences how the scale parameter and the Weibull modulus are strongly affected by the casting conditions. An integrated stochastic-analytical approach is then proposed and it appears to be applicable to describe the tensile properties in terms of fractographic defects and cumulative failure probability P_i.

RIASSUNTO

Nel presente lavoro è stato studiato l'effetto dei difetti sulle proprietà meccaniche di una lega d'alluminio AlSi9Cu3(Fe) pressocolata. È stata realizzata una serie di componenti strutturali con profilo ad U utilizzando una combinazione sistematica dei parametri di iniezione e della temperatura di colata, al fine di generare diversi tipi e quantità di difetti all'interno dei getti. Si è quindi riscontrato che i getti pressocolati contenevano difetti, principalmente porosità e ossidi, e la distribuzione di questi fosse sensibilmente influenzata dalle condizioni di processo utilizzate. Si sono evidenziate, tuttavia, variazioni significative nella distribuzione dei difetti nei componenti realizzati con le medesime condizioni di processo, indicando quindi come i difetti presentino una natura stocastica nei componenti pressocolati. Le proprietà meccaniche sono risultate influenzate dalla quantità e dalla distribuzione dei difetti, e determinate dalla frazione d'area occupata dai difetti stessi sulla superficie di frattura delle provette di trazione. L'influenza dei difetti sulle proprietà meccaniche è stata studiata anche attraverso un approccio teorico basato sull'applicazione di alcuni modelli costitutivi e stocastici. L'approccio analitico, basato sul modello costitutivo di Ghosh, ha indicato correttamente la tendenza dei risultati sperimentali; contemporaneamente il modello statistico di Weibull ha evidenziato come il parametro di scala e il modulo di Weibull sono influenzati sensibilmente dalle condizioni di pressocolata. Un approccio integrato stocastico-analitico è stato quindi proposto e si è dimostrato applicabile per descrivere le proprietà meccaniche in termini di difetti contenuti sulla superficie di frattura e probabilità di rottura P_i.

KEYWORDS

Aluminium alloys; Defects; Oxide films; Porosity; Mechanical properties; Modelling; High pressure die casting.

INTRODUCTION

The unfailing increased use of light alloys in the automotive industry is, above all, due to the need of decreasing vehicle's weight. The same need has to be taken into account in order to face up also both energetic and environmental requirements [1]. In terms of application rates, Al and its alloys have an advantage over other light materials, such as Mg and Ti alloys. The reduced prices, the recyclability, the development of new improved alloys, the increased understanding of design criteria and life prediction for stressed components and an excellent compromise between mechanical performances and lightness are the key factors for the increasing demand of Al alloys. A great contribution to the use of Al alloys comes from improvements in casting processes, which allow to increase the production, to reduce the cycle time, and to manufacture complex-shaped castings with thin wall thickness. Among the recent casting techniques, the high-pressure die-casting (HPDC) is largely used by the automotive sector since fulfils the above advantages [1,2].

A limit to large diffusion of HPDC remains the final quality of castings. While the combination of high speed casting and high cooling rate gives the possibility of thin walled castings, the associated turbulence remains the major source of inner and surface casting defects, which have a deleterious effects on mechanical properties. In HPDC if a number of parameters is not adequately determined and adjusted, the quality of the die cast part results rather poor [3,4]. Macrosegregation of eutectic, primary intermetallic particles [5,6] and α-Al crystals [7], porosity, oxide bifilms and confluence welds [8] are addressed as typical HPDC defects.

By means of casting parameters' adjustments, foundrymen try to restrict and isolate the major part of defects into regions of the casting which are not mechanically stressed during normal working. Further, thin-walled castings, like those produced by HPDC, are more affected by the presence of defects since a single macrodefect can cover a significant fraction of the cross-section area.

A number of researchers has investigated the influence of casting defects on the mechanical properties both of gravity cast [9-13] and high pressure die cast aluminium alloys [14-16]. However, the works of Gokhale *et al.* [17] and Timelli *et al.* [16] evidenced how the mechanical properties decrease monotonically with increasing the area fraction of defects revealed on the fracture surfaces both of gravity and high pressure die cast aluminium specimens. The common conclusion was that even high integrity castings contain defects and thus it is important to predict their effect on final mechanical properties.

In literature, several approaches based on through-process modelling for prediction of the structural behaviour of HPDC magnesium and aluminium alloys components subjected to static and dynamic loads have been suggested [14, 16, 18-20]. Generally, two different routes based on constitutive models [21-23], or statistical and stochastic approaches [11, 24-27] are used. Cáceres [21] and Lee [23] reported that the theoretical approach based on the Ghosh constitutive model [28] can accurately predict the experimental tensile properties of aluminium alloys, even though they used a simple constitutive model. In the model, based upon the tensile instability, the tensile strength and deformation of material with internal discontinuities significantly depend upon the fraction of internal discontinuity, the strain rate sensitivity and strain-hardening ability.

On the other side, the effect of structural defects on mechanical properties have been characterized by Weibull statistics, more specifically, by the two-parameter Weibull modulus [11, 26, 29]. In these early studies, the Weibull modulus appeared to be a useful measure of the reliability of the casting process. Since then, the two-parameter Weibull modulus has been extensively used to characterize the tensile properties, especially the tensile strength. Recently, the use of three-parameter Weibull statistics has been explored to illustrate its superior analytical potential over the traditional two-parameter approach [30]. The three-parameter Weibull analysis provides new information. In particular, minimum values of strength below which the material is extremely unlikely to fail are found.

In the study, the influence of casting defects on mechanical properties of secondary AlSi9Cu3(Fe) die cast alloy was investigated through a systematic experimental approach, with a theoretical verification based on constitutive and stochastic models. Moreover, a combination of injection parameters and pouring temperatures were chosen in order to generate different types and amount of defects throughout the casting.

THEORETICAL ASPECTS

CONSTITUTIVE MODEL OF TENSION INSTABILITY

When porosity or an equivalent defect is present in a tensile specimen, the load bearing area is reduced. Thus, the defective region will yield first, concentrating the strain. The rate of strain concentration can be calculated considering the strain hardening ability of the material. A geometric defect that locally reduces the load bearing area of a tensile specimen results in the formation of an incipient neck. The growth of this neck can be described using the Ghosh constitutive model for the development of plastic instabilities [28]. If the neck is not sharp or the strains involved are not large, it may be considered that only one significant stress exists in either the uniform section or the local inhomogeneity. Under the assumption that the material containing internal discontinuities experiences a tensile load under axial local equilibrium and the effects of strain rate can be neglected, the conventional equation for stress distribution can be expressed in terms of load carrying area as [21, 22, 28]

$$\sigma_i(1 - f)A_0e^{-\varepsilon_i} = \sigma_hA_0e^{-\varepsilon_h} \quad (1)$$

where σ_i, ε_i and σ_h, ε_h are the true stresses and strains in and outside the defect region, respectively, A_0 is the initial cross section of the specimen and f is the area fraction covered by defects.

A numerical solution of eq. (1) can be obtained by means of the following Hollomon constitutive equation [31]

$$\sigma = K\varepsilon^n \quad (2)$$

where σ and ε are the true stress and plastic strain, respectively, while K is the alloy's strength coefficient and n the strain hardening exponent. The substitution of eq. (2) into (1) leads to [21, 22, 28]

$$(1-f)e^{-\varepsilon_i} e_i^n = e^{-\varepsilon_h}\varepsilon_h^n \quad (3)$$

which relates the strain inside the defect region ε_i to the strain outside ε_h.

Moreover, since the true uniform strain of sound material is equivalent to the strain hardening exponent under maximum loading conditions ($\varepsilon_h = \varepsilon = n$), the tensile stress σ_f^*, with a defect content f, can be expressed as the following equation from the power law of eq. (2) [21, 22, 28]

$$\frac{\sigma_f^*}{\sigma^*} = \left(\frac{\varepsilon_h^*}{\varepsilon_h}\right) = \left(\frac{\varepsilon_h^*}{n}\right)^n \quad (4)$$

where σ^* and ε_h are the maximum true stress and maximum strain to fracture of sound material, respectively, and ε_h^* is the premature true strain of material which has a defect content f.

Therefore, the predictions of this model depend on the values of n and f, *i.e.* for a given strain hardening exponent, only the area fraction of defects revealed on the fracture surfaces is important.

WEIBULL STATISTICS

Structural defects such as porosity and oxide inclusions or microstructural features such as Si eutectic or intermetallic phases constitute the initiation point of fracture, since they lead to the largest stress concentration. This point will constitute the weakest link and when the mechanical properties of a group of nominally similar specimens is measured, the data acquired are usually scattered. The statistical distribution that can reasonably model such a distribution was proposed by Weibull [32] and was originally used to analyse the yield strength and fatigue behaviour of steel [33]. The common Weibull distribution function is expressed as

$$P_i = 1 - exp\left[-\left(\frac{\chi-\lambda}{\eta}\right)^{\beta}\right] \quad (5)$$

where P_i is the cumulative fraction of specimen failures (in tensile test); χ is the variable being measured (ultimate tensile strength or elongation to fracture); λ is the threshold parameter, *i.e.* the characteristic stress (or strain) below which no specimen is expected to fail; η is the scale parameter, *i.e.* the characteristic stress (or strain) at which 63.21% of the specimens has failed; β is the shape parameter, alternatively referred to as the Weibull modulus [11,30,32,33]. This configuration of the Weibull distribution is the three-parameter configuration. Generally, for aluminium castings, the two-parameter form is widely adopted and can be expressed with the threshold value λ taken as zero.

The Weibull distribution is asymmetrical about the mean strength (or strain) if compared to Gauss distribution. Simplifying eq. (5) by assuming λ as zero, the Weibull distribution can be converted into the linear form

$$\ln\{\ln[1/(1-P_i)]\} = \beta\ln(\chi) - \beta\ln(\eta) \quad (6)$$

which can be easily plotted with $\ln(\chi)$ and $\ln\{\ln[1/(1-P_i)]\}$ as main axes. If the experimental distribution is Weibullian, a straight line will be produced with slope β and intercept $-\beta\ln(\eta)$. The slope β physically represents the Weibull modulus of the casting, and is clearly a measure of the spread of the distribution [11].

There are a number of statistical criteria that may be used to estimate the probability of failure P_i, such as the modified Kaplan-Meier method, the Herd-Johnson or the Benard methods. The most common approach is the median rank method, alternatively referred to the Benard method [33], which calculates the failure probability P_i as

$$P_i = \left(\frac{i-0.3}{n+0.4}\right) \quad (7)$$

where i is the ranked position of the specimen strength (or strain) in that set of castings and n is the total number of specimens.

EXPERIMENTAL PROCEDURE

The secondary AlSi9Cu3(Fe) cast alloy (EN AC-46000, equivalent to the US designation A380) was supplied as commercial ingots, which were melted in a 500 kg SiC crucible in an electric resistance furnace. Before pouring the melt is held in the furnace at 690 ± 5°C for 1 h to ensure homogeneity and dissolution of the present intermetallic. Periodically, the molten metal was manually skimmed and stirred with a coated paddle to avoid any type of sedimentation. The furnace temperature is the holding temperature commonly used for EN AC-46000 type alloys, which is enough to avoid sludge formation [34,35]. The chemical composition, measured on separately poured samples, is shown in Table 1.

Table 1. Chemical composition of the alloy (wt.%)

Alloy	Si	Mg	Cu	Fe	Mn	Zn	Ni	Cr	Ti	Al
AlSi9Cu3(Fe)	9.87	0.22	2.44	0.76	0.22	0.47	0.06	0.02	0.07	bal.

For R&D purposes, a die for U-shaped casting was made. The CAD model of Al casting with runners, gating and overflow system is displayed in Figure 1. The U-shaped casting with 2.5 mm thickness was coupled with ribs, with ~5 mm thickness, which are generally locations of high defect content. The castings were produced in a Müller-Weingarten cold chamber die-casting machine with a locking force of 7.4 MN. The weight of the Al alloy casting was 3.3 kg, including the runners, gating and overflow system. A detailed description of the HPDC machine, the casting procedure, and the process parameters is given elsewhere [16]. Briefly, 10 to 15 castings were scrapped after the start up, to reach a quasi-steady-state temperature in the shot chamber and die. Oil circulation channels in the die served to stabilize the temperature (at ~230°C). The fill fraction of the shot chamber, with a 70 mm inner diameter, was kept at 0.56. A combination of injection parameters and pouring temperatures were chosen in order to generate different types and amount of casting defects. Table 2 summarizes the

Table 2. Process parameters used for producing U-shaped castings

Process	Plunger velocity slow shot (ms-1)	Plunger velocity fast shot (ms-1)	Switch point (mm)	Intensification pressure (bar)	Melt temperature in crucible (°C)
P1	0.40	3	428	400	690
P2	0.59	3	447	400	690
P3	0.73	2	373	400	690
P4	0.58	2	451	400	690
T2	0.40	3	428	400	640

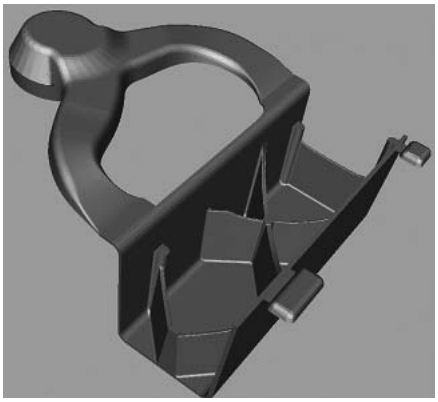

Fig. 1: U-profile casting with gating system: 260 mm length, 110 mm height and 70 mm width. Wall and rib thickness: 2.5 mm and 5 mm, respectively.

process parameters used.

In the P1 reference process, the plunger speed was kept constant in the first phase and a rapid acceleration was applied in the second phase, *i.e.* at the beginning of die filling. The same profile was used for T2 process but the pouring temperature was 50°C lower. In the other shot profiles the plunger was slightly higher in the first phase, minimizing however the air entrapment in the slow shot. The main differences regarded the variations of the switch point between the first and second phase: the commutation point was anticipated in the P3 process and postponed in the P2 and P4 processes. Further, the plunger velocity in the fast shot was reduced in the P3 and P4 profiles. By means of a dynamic shot control system in the HPDC machine, every casting was documented with its shot profile, to monitor the final quality and repeatability. Overall 235 castings were produced with a cycle time of ~115 seconds.

In order to detect the presence of macrodefects, radiographic inspections were carried out throughout the castings and the results have been published previously [16]. This preliminary analysis evidenced how the amount, size and distribution of defects changed by changing the process parameters.

Uniaxial tensile specimens were machined from the wide web, inlet and outlet walls, and ribs of the cast U-profiles as shown in Figure 2, such that the ratio length/width remained the same [16]. Some specimens were machined as aligned with the principal flow direction of the metal during die filling, while others were drawn 90° to the flow direction, as shown in Figure 2. Five sizes of flat tensile specimens were subsequently tensile tested on an MTS 810 tensile testing machine. The crosshead speed used was 2 mm/min ($\dot{\varepsilon} \sim 2 \times 10^{-3}$ s^{-1}). The strain was measured using a 25-mm extensometer. Experimental data were collected and processed to provide yield stress (YS, actually 0.2% proof stress), ultimate tensile strength (UTS) and elongation to fracture (s_f). A total of 160

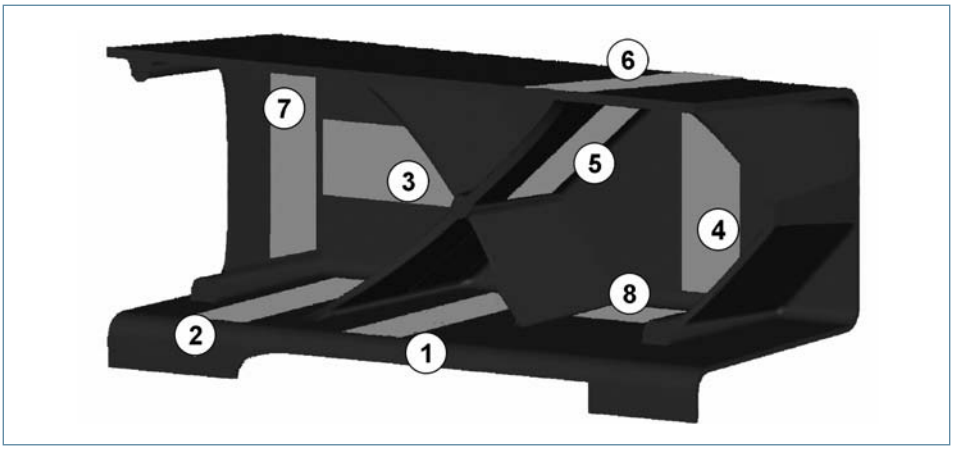

Fig. 2: Illustration of the U-shaped profile showing the investigated locations.

specimens were tested under quasi-static loading conditions at room temperature.

The values of the ultimate tensile strength and elongation to fracture were converted to true tensile strength (σ_f^*) and true plastic strain (ε_h^*) through the following relationships [31]

$$\sigma_f^* = UTS(1+s_f) \quad (8)$$

$$\sigma_h^* = ln(1+s_f) \quad (9)$$

Finally the Quality Index, Q, was calculated as [36]

$$Q = UTS + 0.4 \cdot K \cdot \log(100 \cdot s_f) \quad (10)$$

where K is the alloy's strength coefficient.

The analysis of the fractured surfaces was carried out using an optical stereomicroscope and a scanning electron microscope (SEM). The acquired images were then transferred into a single photograph and the area of defects was quantitatively analyzed using an image analyzer (Leica LAS). The total measured defect area was then divided by the initial cross section of the tensile specimen to find the defect area fraction. In order to study the influence of casting defects on mechanical properties, the previously described constitutive and stochastic approaches were then applied and discussed.

RESULTS AND DISCUSSION

ANALYSIS OF FRACTURE SURFACES

It was found that the U-shaped castings contain defects, primarily pores and oxides, and that the presence and distribution of these defects are highly sensitive to the process conditions. Significant variations of defect distribution were, however, found in castings produced under the same conditions, indicating the stochastic nature of defects in die castings [16]. The number of defects revealed on fracture surfaces varied between 2 and 20. The presence of porosity is mainly ascribed to gas entrapment phenomena during the die filling and to the blockage of vents due to the premature solidification of the molten metal. Generally, the gas pores showed a deformed spherical shape with shiny oxidized surface, while oxides appeared as rough and dull regions on the fracture surface. The presence of cold shots was also observed, generally, incorporated within porosity (Figure 3). Contrary, sound specimens revealed a fracture mode predominantly intergranular with regions of cleavage facets, which are visible in the silicon precipitates and brittle intermetallic phases, and with zones of deformed and fractured micronecks of α-Al solid solution (Figure 4). The fracture path follows mainly the interdendritic eutectic zone.

As previously observed by Cáceres and Selling [22], the fracture surfaces were flat, although a certain degree of tortuosity was present. Therefore, trying to determine exactly if a particular defect was intersected by the fracture plane or the locus of the actual intersection was a rather arbitrary exercise. The determination of area fraction covered by defects was particularly critical for oxides, which were sometimes sitting along the main axis of tensile specimens, as shown in Figure 5. Thus, it was assumed that all visible defects on the fracture surface lied on a single cross sectional plane and the projected area was considered for the calculation.

APPLICATION OF THE CONSTITUTIVE MODEL

From tensile testing, it was observed how, considering the same investigated location of the casting, the mechanical properties, such as UTS and elongation to fracture, showed different values by changing process parameters; while, fixing the process variables, the mechanical properties changed throughout the casting. Details of mechanical properties and quality maps of diecast components are provided elsewhere [16].

In general, it was possible to observe how the different amount of defects revealed on the fracture surface influenced the tensile properties, such as UTS and elongation to fracture. As reported in Ref. 16, 21, 22 and 28, defects considerably influence the plastic tensile properties of the material but not the elastic ones. Thus, the Young modulus (E) and the YS were steady at ~72 GPa and ~177 MPa, respectively. The initial yield stress is largely determined by the relatively high supersaturation of atoms (Mg, Cu and Si) in α-Al matrix, which is referred to the high solidification rate.

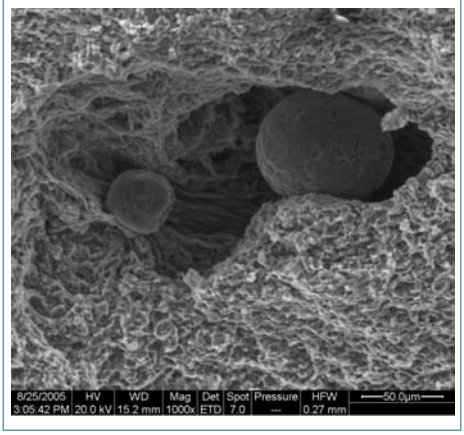

Fig. 3: SEM micrograph of gas porosity with entrapped cold shots as revealed on fracture surface.

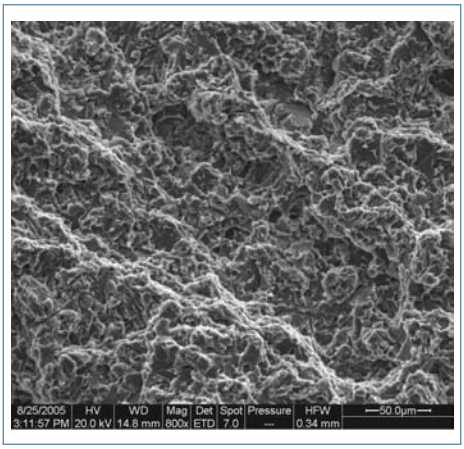

Fig. 4: SEM view of the fracture surface of sound specimens.

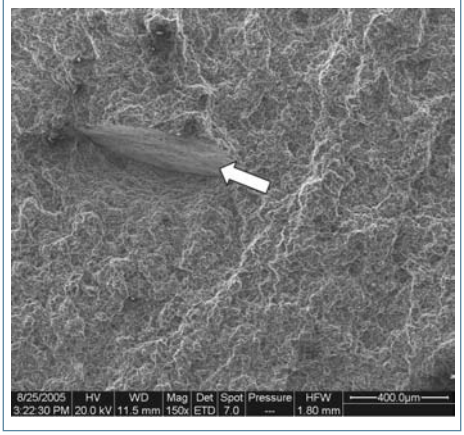

Fig. 5: SEM micrograph of oxide film on the fracture surface of sample lying almost perpendicular to the fracture plane.

The *n* and *K* values were determined by using a double logarithmic plot of the true stress and the true plastic strain, where the *n*-value represents the slope and the *K*-value corresponds to the true stress at a true strain value of unity. No relation between the defect content and the strength coefficient seems to exist, suggesting how the strength coefficient is a matrix controlled parameter. Cáceres [36] reported how the strength coefficient relates to the YS as

$$k = YS \left(\frac{E}{\alpha \cdot YS} \right)^{n} \qquad (11)$$

where E is the Young modulus and α a scale factor.

Evaluating the studied alloy in terms of strain hardening exponent, it is observed that the amount of defects does not influence the plastic deformation rate, which is mainly controlled by the microstructure scale, such as secondary dendrite arms spacing [37]. The calculated *n* and *K* values were steady at 0.23 and 755 MPa, respectively.

As shown in Figure 6, the relations between the tensile properties and fractographic defects exhibit good agreement with the overall regression of experimental results. The true tensile strength (σ_f^*) of the alloy exhibits a linear dependence that decreases from 310 to 160 MPa as the area fraction of defects increases up to about 23%. Further, the true plastic strain (ε_i^*) decreases drastically from ~2.1 to 0.3% on an inverse parabolic relationship with the increase in defect level.

Figure 6 shows a comparison between the constitutive prediction and the experimental results of the σ_f^* (6a) and ε_i^* (6b), in terms of variation of area fraction of defects. The true elongation to fracture of the most ductile specimen (ε_i^*) was 0.021 and it was used in the constitutive model to find the maximum homogeneous strain, ε_h^*, for the different *f*-values in eq. (3). Contrary to the Cáceres' work [21], the values of true tensile strength were not normalised as defined by eq. (4), but the effect on the tensile strength was calculated using eq. (2), with n = 0.23, K = 755 MPa and the ε_h^* values from eq. (3). As shown the calculated curves correctly indicate the trends of the experimental results.

Figure 7 evidences how the relation between the Quality Index and the area fraction of defects shows a good agreement with the overall regression result. The Quality Index exhibits a linear dependence that decreases from 370 to 35 MPa by increasing the *f*-value.

In order to model the influence of casting defects on the Quality Index, Q, eqs. (8) and (9) have been substituted into eq. (10), leading to

$$Q=\frac{(\varepsilon_h^*)}{\exp(\varepsilon_h^*)}+0.8\cdot K+\log\left[\exp(\varepsilon_h^*)-1\right] \quad (12)$$

which relates the Quality Index, Q, to the maximum homogeneous strain, ε_h^*, for the different *f*-values. The calculated Q-values (joined by the solid line) as a function of area fraction of defects are compared with the experimental results in Figure 7. As shown the calculated curve correctly indicate, yet again, the trend of the experimental data.

The results shown in Figures 6 and 7 indicate how the area fraction of defects evaluated in the fracture surface is a reliable parameter to predict the tensile properties of the material, despite some scatter in the data. The results are also in good agreement with the analytical approach based on the Ghosh constitutive model. The scatter observed in the experimental data can be considered, at least in part, as inherent to the fracture behaviour of the material [22]. Some imperfections are always present, even in sound specimens, which tend to show some vertical scatter in tensile strength and ductility [38]. The source of horizontal scatter arises from the measurements of the defect size since the boundaries of defects

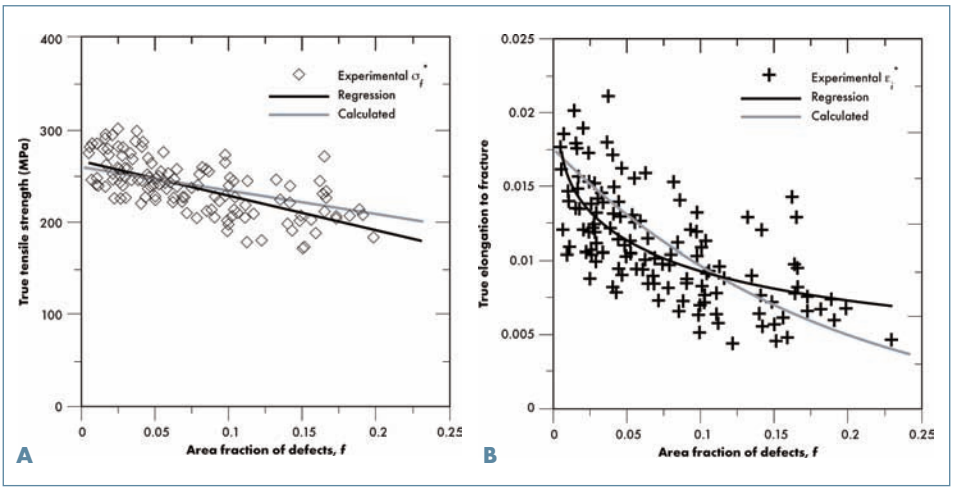

Fig. 6: (a) The true tensile strength and (b) the true elongation to fracture as a function of the area fraction of defects in the fracture surface. The solid lines represent the regression and the calculated curves using the constitutive model of tension instability explained in §2.1.

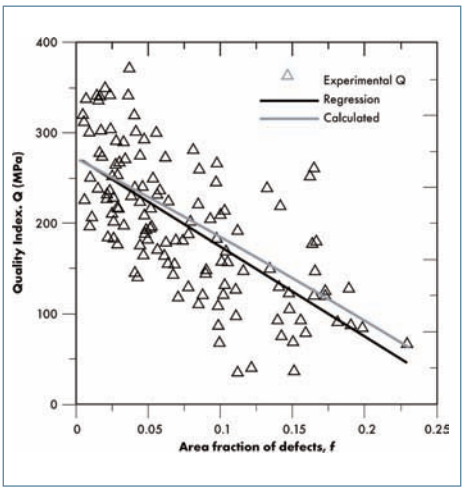

Fig. 7: The Quality Index, Q, as a function of the area fraction of defects in the fracture surface. The solid lines represent the regression and the calculated curves obtained according to eq. (12).

were often ill-defined, making the quantification of the area of defects an arbitrary exercise. A related and more significant effect can be attributed to the fact that defects do not always lie on the same cross sectional plane, especially oxides, and therefore the projected area used to calculate *f* may be overestimated respect to the real defect area fraction.

Several works [13,39,40] suggested that the morphology and the distribution of defects are important factors controlling the final mechanical properties. Thus, there is the possibility that some of the scatter can be attributed to these causes.

In the present work, tensile specimens with an area fraction of defects higher than ~0.23 presented a brittle fracture well below the yield point. This means that the strain concentration in the defective region produces a very high damage rate of brittle particles within the microstructure, causing the premature fracture of the specimen. In sound Al-Si specimens, the tensile fracture generally occurs at a constant level of damage in the form of cracked eutectic Si particles, about 15% of the total particles' population [41].

APPLICATION OF WEIBULL STATISTICS

The frequency distributions of UTS and s_f for the five process parameters used to produce the U-shaped castings were plotted and analysed. The tensile strength and elongation to fracture data were analyzed using both the Gauss and the two-parameter Weibull models for which the parameters were estimated by the maximum likelihood method. The goodness of fit for each distribution was evaluated by the modified Anderson-Darling test, A^2. The test statistics for each fit showed that the fitted distribution could not be rejected. In general, the correlation coefficient, R^2, of the Weibull distributions calculated for the different processes is higher than ~0.98, while it is around 0.95 considering the Gauss distributions. This makes the use of the Weibull statistical approach as reliable. As shown in Figure 8, which refers to the P1 process, both the distributions of UTS and s_f are skewed about the mean values and

they are better fitted by the Weibull distribution function than by Gauss one.
Figure 9 shows the corresponding Weibull plots where the diameter of the bubbles is proportional to the area fraction of defects evaluated in the fracture surface of the tensile specimens. While lower values in the two plots represent the specimens with the highest *f* values, the diameter of the bubbles decreases along the straight lines. Therefore, the probability of failure P_i increases by increasing the defect content *f*, indicating the fundamental role of defects on fracture mechanism.
Table 3 shows the quantitative results of the Weibull analysis of the AlSi9Cu3(Fe) alloy cast with different process parameters. It is evident how the β and η values for the two-parameter fits are strongly affected by the casting parameters used. The results show that the Weibull moduli for the UTS and elongation to fracture of the P1 reference process were 9.2 and 3.3, respectively, but changing the injection profiles, as done in the P2, P3 and P4 processes, caused the Weibull moduli to decrease. The reduction of the casting temperature from 690 to 640°C in the P1 process caused a reduction of the Weibull moduli for UTS and elongation to fracture to 6.5 and 2.5, respectively. The minimum β values were reached by using the P4 process. This means that reducing the plunger velocity during the fast shot and simultaneously delaying the commutation point between first and second phase clearly decreases the reliability of the castings.
Concerning the scale parameter η for UTS and elongation to fracture, the highest values were reached by the P2 process, that is 256 MPa and 1.35%, respectively, while the lowest values were obtained with the P3 process where 63.21% of the specimens has failed at 230 MPa and 1.05%. These values and the highest mechanical properties reached in the work are well below the maximum mechanical properties attainable for AlSi9Cu3(Fe) alloys. Recently, Gunasegaram et al. [42] and Timelli et al. [43] evidenced how EN AC-46000 type alloys can reach values of 320 MPa for UTS and ~4% as elongation to fracture, if the defect content is significantly reduced.
In AlSi5Cu3Fe1Mg0.3 alloys modified with Mn or Sr, Zahedi et al. [30] observed that in a two-parameter Weibull plot there exists a threshold stress λ below which failure would not occur, suggesting that three-parameter Weibull analysis would be more appropriate. When λ is taken as zero, as in the two-parameter fits, there is a probability that the fracture stress of specimens will be less than the yield stress, even if the specimen has reached and deformed plastically beyond the yield stress. It is important to underline that in the two-parameter Weibull model, the ratio of the average to the standard deviation is a function only of β as follows

$$\frac{\bar{\sigma}}{S_\sigma} = \frac{\Gamma\left(1+\frac{1}{\beta}\right)}{\sqrt{\Gamma\left(1+\frac{2}{\beta}\right)-\left(\Gamma\left(1+\frac{1}{\beta}\right)\right)^2}} \qquad (13)$$

where $\bar{\sigma}$ is the average fracture stress, S_σ is the standard deviation, and Γ represents the gamma function. Increases in the average or decreases in the standard deviation increase the value of the Weibull modulus. Hence, higher β does not necessarily mean higher repeatability or reliability [30].
In this work, for both UTS and elongation to fracture, however, the two-parameter Weibull was more appropriate as the three-parameter fits yielded negative threshold values or around zero.
Therefore, increases in β observed previously by changing HPDC process parameters and using two-parameter Weibull statistics could be probably considered as "an increase in safety" more than "an increase in reliability", because it would indicate an increase in the threshold stress or elongation to fracture if three-parameter Weibull statistics were used.

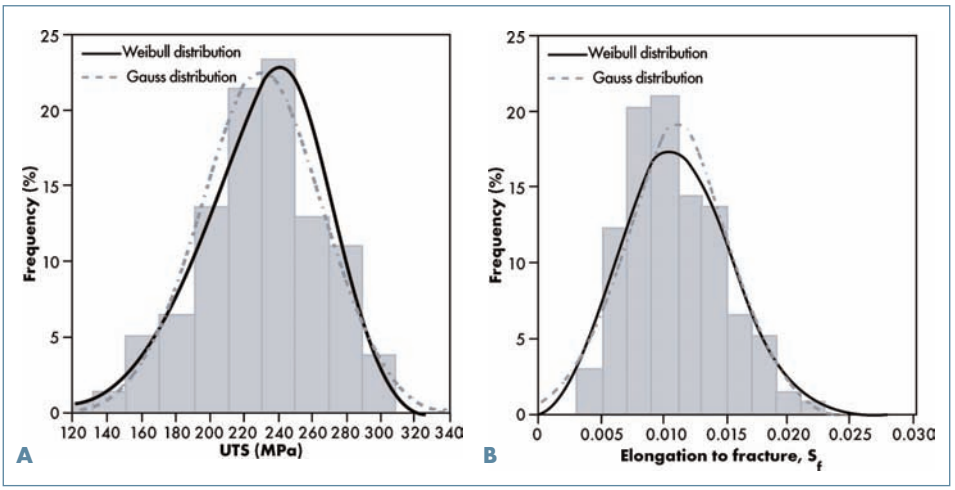

Fig. 8: Histograms of (a) ultimate tensile strength and (b) elongation to fracture distributions referred to the P1 process. The Weibull and Gauss distribution functions are superimposed.

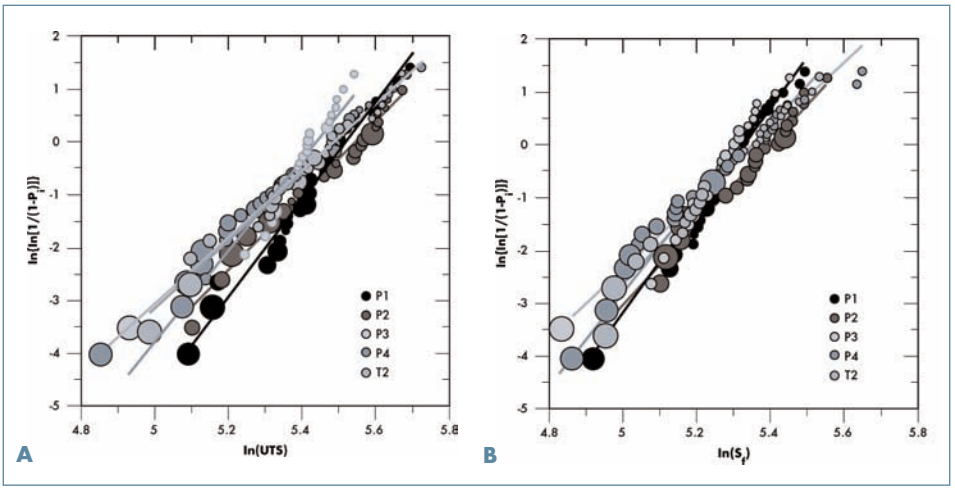

Fig. 9: Weibull plots for UTS and elongation to fracture values obtained from different casting processes; the diameter of each bubble is proportional to the area fraction of defects *f*.

AN INTEGRATED STOCHASTIC-ANALYTICAL APPROACH

The analytical approach based on the Ghosh constitutive model and the stochastic approach based on the Weibull statistics were integrated for the true tensile strength and true elongation to fracture. The tensile properties, fractographic defects and cumulative failure probability P_i were correlated in Figure 8 by using 2D contour plots, which were plotted by using the Systat® v.11 software. The software first computes its own square grid of interpolated or directly estimated values. From this grid, contours are followed using the Lodwick-Whittle method combined with linear interpolation. This method is guaranteed to find proper contours if the grid is fine enough [44]. Thus, maps of iso-probability failure are generated for the tensile properties of AlSi9Cu3(Fe) alloy. Furthermore, the calculated curves using the constitutive model of tension instability were plotted as solid lines in Figure 8 to fit the experimental results, where each point is parametric to P_i value. Now, it is possible to observe how 63.21% of the overall tensile specimens has failed at scale values of ~245 MPa and ~1.2%, for σ_f^* and ε_i^* respectively. By intercepting the calculated solid curves, these values correspond to a defect area fraction f equal to ~0.06. From another point of view, this means that tensile specimens die cast with AlSi9Cu3(Fe) alloy and with an area fraction of defects lower than ~6% have a survival probability of 36.79%.

Table 3. Weibull moduli, β, and scale parameters, η, for UTS and elongation to fracture values obtained from different casting processes; coefficients of determination, R^2, are given.

	UTS			s_f		
Process	β	η (MPa)	R^2	β	η (%)	R^2
P1	9.2	249	0.99	3.3	1.10	0.99
P2	7.1	256	0.99	2.6	1.35	0.99
P3	8.7	230	0.97	3.0	1.05	0.98
P4	6.3	243	0.99	2.2	1.21	0.98
T2	6.5	243	0.99	2.5	1.18	0.99

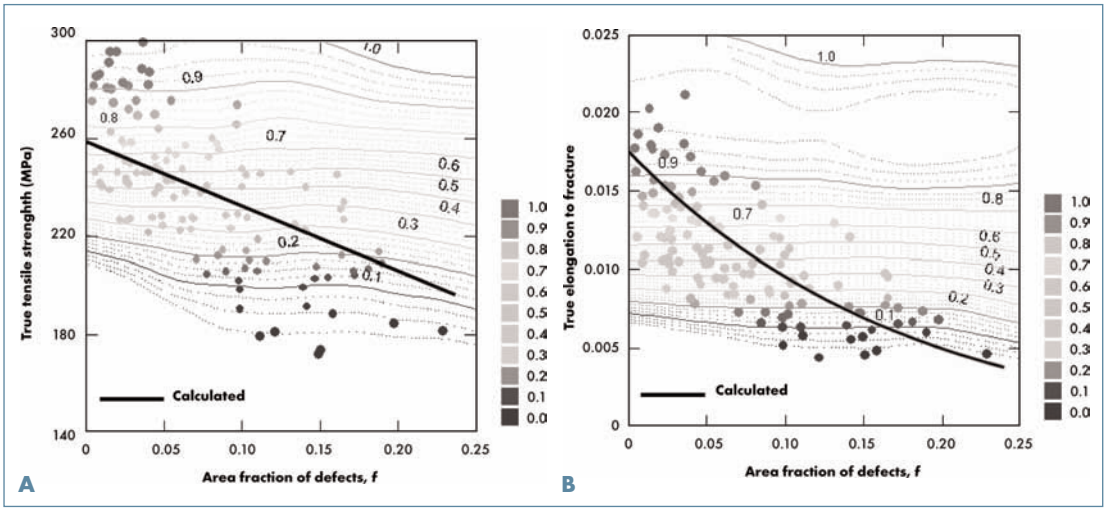

Fig. 10: Contour plots of (a) true tensile strength and (b) the true elongation to fracture as a function of the area fraction of defects in the fracture surface. Each point is parametric to the cumulative failure probability P_i value. The solid lines represent the calculated curves using the constitutive model of tension instability.

CONCLUSIONS

The influence of casting defects on mechanical properties of a high pressure die cast AlSi9Cu3(Fe) has been investigated through a systematic experimental approach, with a theoretical verification based on constitutive and stochastic models. Based on the results obtained in the study, the following conclusions can be drawn.

- U-shaped components diecast with a combination of different injection parameters and pouring temperatures show defects mainly in the form of pores and oxides.
- The presence and distribution of these defects are highly sensitive to the process conditions. Significant variations of the defect amount and distribution are, however, found in castings produced under the same conditions, indicating the stochastic nature of defects.
- The different type and amount of defects influence considerably the plastic tensile properties of the material, such as the ultimate tensile strength and elongation to fracture, but not the elastic characteristics.
- The relations between the tensile properties and the area fraction of defects revealed on the fracture surfaces exhibit good agreement with the overall regression of experimental results.
- The analytical approach based on the constitutive model of tension instability correctly indicate the trends of the experimental results.
- The Weibull statistics evidenced how the scale parameter η and the Weibull modulus β are strongly affected by the diecasting parameters used, and therefore by the overall amount of defects.
- An integrated stochastic-analytical approach appears to be used to describe the tensile properties in terms of fractographic defects and cumulative failure probability P_i.

ACKNOWLEDGEMENTS

This work was developed with the financial support of the European Projects NADIA (New Automotive components Designed for and manufactured by Intelligent processing of light Alloys, NMP-2004-SME 3.4.4.5, contract n.026563-2) and IDEAL (Integrated Development Routes for Optimised Cast Aluminium Components, contract n.GRD2-2001-50042). The author would like to acknowledge the skilful contribution of Audi GmbH for high pressure die castings and Dr. M. Sadocco and Dr. A. Urbani for the experimental support to this research. Many thanks are also due to the "mud angels" of DTG for their extraordinary work after the great flood of Vicenza.

REFERENCES

[1] Valentini, G.. Proceedings of the International Conference High Tech Die Casting, Vicenza, Italy, February 22, 2002, pp. 237-250.

[2] Wagner, V.. Proceedings of the International Conference High Tech Die Casting, Vicenza, Italy, February 22, 2002, pp. 1-42.

[3] Syrcos, G.P. Die casting process optimization using Taguchi methods. J. Mater. Process. Technol., 135 (2003), pp. 68-74.

[4] Verran, G.O., R.P.K. Mendes and M.A. Rossi. Influence of injection parameters on defects formation in die casting Al12Si1.3Cu alloy: Experimental results and numeric simulation. J. Mater. Process. Technol., 179 (2006), pp. 190-195.

[5] Laukli, H.I., C.M. Gourlay and A.K. Dahle. Effects of Si content on defect band formation in hypoeutectic Al-Si die castings. Mat. Sci. Eng. A, 413-414 (2005), pp. 92-97.

[6] Timelli, G. and F. Bonollo. The influence of Cr content on the microstructure and mechanical properties of AlSi9Cu3(Fe) die casting alloys. Mat. Sci. Eng. A, 528 (2010), pp. 273-282.

[7] Laukli, H.I., C.M. Gourlay and A.K. Dahle. Migration of crystals during the filling of semi-solid castings. Met. Mater. Trans. A, 36 (2005), pp. 805-818.

[8] Gariboldi, E., F. Bonollo and P. Parona. In Handbook of defects in high pressure diecastings, AIM, Milano, 2010.

[9] Campbell, J. In Elsevier (Ed.), Castings, 2nd ed., Butterworth-Heinemann, Oxford, 2003.

[10] Dai, X., X. Yang, J. Campbell and J. Wood. Effects of runner system design on the mechanical strength of Al-7Si-Mg alloy castings. Mater. Sci. Eng. A, 354 (2003), pp. 315-325.

[11] Dai, X., X. Yang, J. Campbell and J. Wood. Influence of oxide film defects generated in filling on mechanical strength of aluminium alloy castings. Mater. Sci. Technol., 20 (2004), pp. 505-513.

[12] Wang, Q.G., D. Apelian and D.A. Lados. Fatigue behavior of A356-T6 aluminum cast alloys. Part I. Effect of casting defects. J. Light Met., 1 (2001), pp. 73-84.

[13] Francis, J.A. and G.M.D. Cantin. The role of defects in the fracture of an Al-Si-Mg cast alloy. Mater. Sci. Eng. A, 407 (2005), pp. 322-329.

[14] Avalle, M., G. Belingardi, M.P. Cavatorta and R. Doglione. Casting defects and fatigue strength of a die cast aluminium alloy: A comparison between standard specimens and production components. Int. J. Fatigue, 24 (2002), pp. 1-9.

[15] Aziz Ahamed, A.K.M., H. Kato, K. Kageyama and T. Komazaki. Acoustic visualization of cold flakes and crack propagation in aluminum alloy die-cast plate. Mater. Sci. Eng. A, 423 (2006), pp. 313-323.

[16] Timelli, G. and F. Bonollo. Quality mapping of aluminium alloy diecastings. Metal. Sci. Tech., 26 (2008), pp. 2-8.

[17] Gokhale, A.M. and G.R. Patel. Origins of variability in the fracture-related mechanical properties of a tilt-pour-permanent-mold cast Al-alloy. Scripta Mater., 52 (2005), pp. 237-241.

[18] Greve, L.. Proceedings of the Sixth International Conference Magnesium Alloys and their Applications, DGM, Wolfsburg, Germany, 2003, pp. 789-802.

[19] Dørum, C., O.S. Hopperstad, O.-G. Lademo and M. Langseth. Numerical modelling of the structural behaviour of thin-walled cast magnesium components using a through-process approach. Mater. Des., 28 (2007), pp. 2619-2631.

[20] Dørum, C., H.I. Laukli and O.S. Hopperstad. Through-process numerical simulations of the structural behaviour of Al-Si die-castings. Comput. Mater. Sci., 46 (2009), pp. 100-111.

[21] Cáceres, C.H.. On the effect of macroporosity on the tensile properties of the Al-7%Si-0.4%Mg casting alloy. Scripta Metall. Mater., 32 (1995), pp. 1851-1856.

[22] Cáceres, C.H. and B.I. Selling. Casting defects and the tensile properties of an Al-Si-Mg alloy. Mater. Sci. Eng. A, 220 (1996), pp. 109-116.

[23] Lee, C.D.. Effects of microporosity on tensile properties of A356 aluminum alloy. Mater. Sci. Eng. A, 464 (2007), pp. 249-254.

[24] Khan, M.I., Y. Frayman and S. Nahavandi. InTech'03 Proceedings of the Fourth International Conference on Intelligent Technologies 2003, 17-19 December 2003, Chiang Mai Plaza, Thailand.

[25] Espinoza-Cuandra, J., G. García-García and H. Mancha-Molinar. Influence of defects on strength of industrial aluminum alloy Al-Si 319. Mater. Des., 28 (2007), pp. 1038-1044.

[26] Dispinar, D. and J. Campbell. Use of bifilm index as an assessment of liquid metal quality Int. J. Cast Metals Res., 19 (2006), pp. 5-17.

[27] Dørum, C., O.S. Hopperstad, T. Berstad and D. Dispinar. Numerical modelling of magnesium die-castings using stochastic fracture parameters. Eng. Fract. Mech., 76 (2009), pp. 2232-2248.

[28] Ghosh, A.K.. Tensile instability and necking in materials with strain hardening and strain-rate hardening. Acta Metall., 25 (1977), pp. 1413-1424.

[29] Green, N.R. and J. Campbell. Statistical distributions of fracture strengths of cast Al-7Si-Mg alloy. Mater. Sci. Eng. A, 137 (1993), pp. 261-266.

[30] Zahedi, H., M. Emamy, A. Razaghian, M. Mahta, J. Campbell and M. Tityakio_lu. The effect of Fe-rich intermetallics on the Weibull distribution of tensile properties in a cast Al-5 Pct Si-3 Pct Cu-1 Pct Fe-0.3 Pct Mg alloy. Met. Mater. Trans. A, 38 (2007), pp. 659-670.

[31] Dowling, N.E.. In Mechanical behavior of materials - Engineering methods for deformation, fracture, and fatigue. Prentice Hall, 2nd ed., Upper Saddle River (NJ), 1999.

[32] Weibull, W.. A statistical distribution function of wide applicability. J. Appl. Mech., 18 (1951), pp. 293-297.

[33] Weibull, W.. In Fatigue testing and analysis of results, Pergamon Press, Oxford, 1961, pp. 159-199.

[34] Casting Eng., 11/12 (1986), pp. 30-36.

[35] Gobrecht, J.. Gravity Segregation of Iron, Manganese, and Chromium in Al-Si Casting Alloys - 1. Giesserei, 61 (1975), pp. 263-265.

[36] Cáceres, C.H.. A Phenomenological Approach to the Quality Index of Al-Si-Mg Casting Alloys. Int. J. Cast Metals Res., 12 (2000), pp. 367-375.

[37] Seifeddine, S., S. Johansson and I.L. Svensson. The influence of cooling rate and manganese content on the β-Al5FeSi phase formation and mechanical properties of Al-Si-based alloys. Mater. Sci. Eng. A, 490 (2008), pp. 385-390.

[38] EN 12258-1, Aluminium and Aluminium alloys – Terms and Definitions, UNIMET, 2001.

[39] Buffière, J-Y., S. Savelli, P.H. Jouneau, E. Maire and R. Fougères. Experimental study of porosity and its relation to fatigue mechanisms of model Al-Si7-Mg0.3 cast Al alloys. Mater. Sci. Eng. A, 316 (2001), pp. 115-126.

[40] Shan, Z. and A.M. Gokhale. Micromechanics of complex three-dimensional microstructures. Acta mater., 49 (2001), pp. 2001-2015.

[41] Cáceres, C.H. and J.R. Griffith. Damage by the cracking of silicon particlesin an Al-7Si-0.4Mg casting alloy. Acta Mater., 44 (1996), pp. 25-33.

[42] Gunasegaram, D.R., B.R. Finnin and F.B. Polivka. Effect of flow velocity on the properties of high pressure die cast Al-Si alloy. Mater. Forum, 29 (2005), pp. 190-195.

[43] Timelli G., S. Ferraro, F. Grosselle, F. Bonollo, F. Voltazza and L. Capra, Proceedings of the 33° AIM National Conference, Brescia, Italy, November 10-12, 2010, paper no. 118 (on CD).

[44] Systat Tutorials, Systat® 11.0.0.1.